ACS SENSORS

Cite This: *ACS Sens.* 2019, 4, 2638−2645

pubs.acs.org/acssensors

Adhesive Tape Microfluidics with an Autofocusing Module That Incorporates CRISPR Interference: Applications to Long-Term Bacterial Antibiotic Studies

Taejoon Kong,[†,§] Nicholas Backes,[‡,§] Upender Kalwa,[†] Christopher Legner,[†] Gregory J. Phillips,[*,‡] and Santosh Pandey[*,†]

[†]Electrical and Computer Engineering and [‡]Veterinary Microbiology and Preventive Medicine, Iowa State University, Ames, Iowa 50011, United States

[*] *Supporting Information*

ABSTRACT: The ability to study bacteria at the single cell level has advanced our insights into microbial physiolo as the resting substrate, along with a temperature-controlled environmental chamber, allows the culturing of ba

KEYWORDS: microfluidics, bacteria, single cell, antibiotics, gene expression, CRISPR interference

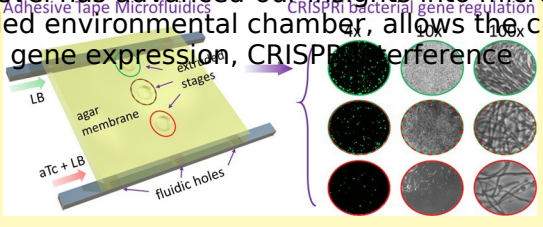

The emergence of bacterial antibiotic resistance (AMR) has become an alarming threat to global public health.[1] Consequently, new strategies are sought to improve the effectiveness of antibiotics in current clinical use, as well as to identify new targets for antimicrobial agents.[2−5] One challenge toward combatting AMR lies in the inherent heterogeneity of bacterial cells at the population level∂be it in cell growth and division, gene expression, or mutation rates.[4,6,7] This can make it challenging to identify new strategies to eliminate bacterial pathogens.[8,9] Fortunately, rapid progress in engineering technologies, including development of sensitive chemical probes, new devices for monitoring microbial growth imaging single cells, instrumentation, robotics, optics, and data analytics, along with synthetic biology offers new opportunities to address the human and animal health concerns of AMR.[10−13]

For example, bacterial assays with a higher throughput are needed that can more rapidly screen for AMR levels and new cellular targets for further interrogation. Currently, bacterial

evolving heterogeneity in microcolonies.[14] Alternatively, microfluidic assays enable the growth of linear or monolayer colonies with time-lapsed imaging.[15−17] Three-dimensional culture of bacterial biofilms and aggregates have also been demonstrated.[18−21] However, the fabrication of silicon or SU8 master molds requires access to a clean room and advanced lithography equipment and is not cost-effective for repeated experiments.[9,22−24] In this context, droplet microfluidics is a promising technique for the confinement of single cells within individual compartments, each having a distinct chemical signature.[8,25] Droplet microfluidics offers the possibility of creating parallel droplets with iterative operations of merging, mixing, sorting, and incubation of cells for extended time periods.[8,26] However, droplet microfluidics has its set of challenges for bacterial studies, such as maintaining a stable concentration of oxygen and other gases, providing media perfusion during cell incubation, and minimizing cross- contamination or exchange of material between droplets.[8] In addition, most of the droplet microfluidics research uses

culture studies are generally performed in Petri dishes and multiwell plates for their simplicity, low-cost, and ease of handling. However, plate assays make it difficult to replenish media, track the lineage of growing cells or observe the

Received: June 4, 2019
Accepted: October 4, 2019
Published: October 4, 2019

DOI: 10.1021/acssensors.9b01031

fluorescence labeling or fluorescent protein expressing cells which limits the technology to engineered strains.[8] To overcome these limitations, resazurin bacterial indicator dye is used in digital droplet microfluidics which reduces to a strongly fluorescent resorufin molecule in the presence of intracellular electron receptors.[27−29] In this paper, we present a novel microfluidic platform for long-term, bacterial antibiotic studies that comprised a low-cost microfluidic device and real- time autofocusing module. (i) The microfluidic device was made by stacking multiple patterned layers (i.e., double-sided adhesive tape, transparency film, agarose membrane, and coverslip) onto the glass substrate (Figure 1). No silicon microfabrication or polymer processing steps were used, which is appealing for wider adoption to microbiologists. Bacterial cells were immobilized on the agarose membrane and exposed to fresh media or antibiotics through side channels. (ii) The autofocusing module enables extended time-lapse imaging by self-correcting for any *z*-direction focal plane movements that can blur the recorded image. The module consists of a software script and hardware components (i.e., stepper motor, micro- controller, and knob attachment) that monitor the focus measure of captured images at real-time and adjust the microscope's focus as required. Multiple $x-y$ points were imaged by manual positioning of the microscope stage using reference features on the agarose membrane. The combination of low-cost microfluidics and autofocusing module allowed us to observe cell growth and division, quantify the minimum inhibitory concentration (MIC), and reveal morphological changes in the bacteria. To facilitate identification of new genetic determinants of antibiotic susceptibility, we further tailored our system to achieve precise, titratable control of gene expression by CRISPR interference (CRISPRi).

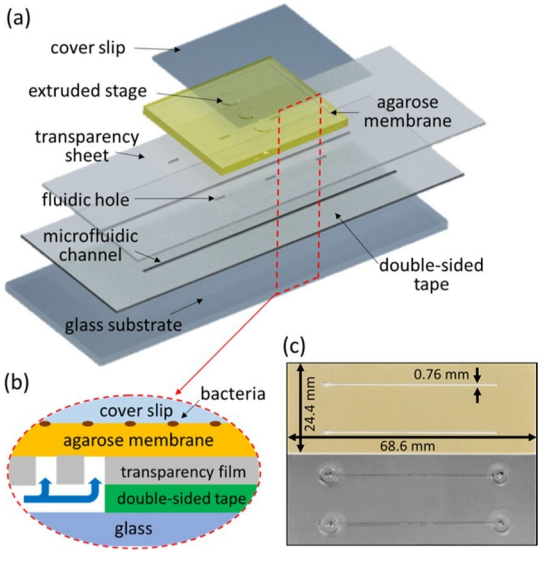

Figure 1. Three-dimensional view of the microfluidic device for bacterial CRISPRi studies. (a) Device was constructed on a glass substrate by stacking multiple layers (i.e., double-sided adhesive tape, transparency film, agarose membrane, and coverslip). (b) Cross- sectional view of the assembled device is shown. The media or antibiotic solution was flown through the microfluidic channels which diffused into the agarose membrane through fluidic holes created in the transparency film. Thereafter, bacterial cells cultured on the agarose membrane were exposed to the solution. (c) Image of the actual microfluidic device after the assembly of different layers.

EXPERIMENTAL SECTION

Materials and Equipment. Lysogeny broth (LB) (10 g of

DOI: 10.1021/acssensors.9b01033

tryptone, 5 g of yeast extract, 10 g of NaCl/L) was obtained from Thermo Fisher Scientific (catalog #10855021, Dubuque, IA). Fluorescein (MW 332 mol^{-1}) was purchased from Sigma-Aldrich (Catalog #F2456, St. Louis, MO). A polydimethylsiloxane (PDMS) prepolymer and curing agent were obtained from Ellsworth Adhesives (Dow SYLGARD 182 Silicone Encapsulant Clear 0.5 kg Kit, Germantown, WI). A high melting temperature agarose was purchased from Alfa Aesar (catalog #9012-36-6, Tewksbury, MA). The microfluidic devices were constructed using a glass slide (catalog #12-540-C, Thermo Fisher Scientific, Pittsburg, PA), double-sided adhesive transfer tape (3M, catalog #9474LE 300LSE, Maplewood, MN), and transparency film (Staples Inc., catalog #21828, Ames, IA) (Figure 1a). An upright student microscope (Leica DM 500) with a CCD camera (QImaging QICAM Fast 1394) was used to take images of bacterial cells (Leica Camera, Wetzlar, Germany) (Figure 2a). An

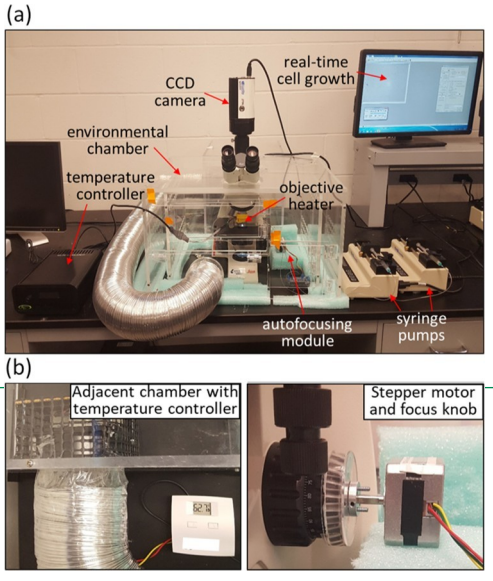

Figure 2. Setup for long-term bacterial cell imaging. (a) Phase contrast optical microscope was placed inside an environmental chamber along with a CCD camera, temperature controller, objective heater, syringe pump, and autofocusing module. The user can remotely adjust the focus knob and monitor the bacterial growth on the computer monitor. (b) Heater fan with temperature controller was installed in an adjacent chamber to regulate the ambient temperature. A stepper motor, operated by a microcontroller, was attached to the focus knob to automatically maintain the focus of recorded images over long time periods.

upright stereozoom fluorescent microscope (Leica MZ 16) with a 470 nm GFP filter cube and external light source (Leica EL 6000) were used for fluorescein measurements (Leica Camera, Wetzlar, Germany). A temperature controller (TC-1-100), heating plate (TC-GSH), and objective heater (TC-HLS-05) were purchased from Bioscience Tools (online vendor). The environmental chamber was designed in AutoCAD and constructed by Country Plastics (Ames, IA). A fan heater (IncuKit) was purchased from Incubator Warehouse (online vendor). The syringe pumps (KDS 250) were purchased from KD Scientific Inc. (Holliston, MA).

Microfluidic Device Design and Fabrication.

Microfluidic channels were designed in Silhouette Studio (Silhouettte America Inc., Lindon, Utah). Their Silhouette Cutting Machine (Silhouette Cameo 3) was used to scribe the adhesive tape (Figure 1c). The prepared tape was attached to a glass slide using the edge of the slide as a reference. The transparency film comprising input/output ports and fluidic holes was placed on top using the microfluidic channels as

DOI: 10.1021/acssensors.9b01033

reference (Figure 1b). Solidified PDMS was punched using a 4 mm biopsy punch (BP40, HealthLink Inc., Jacksonville, FL) with each cylindrical PDMS piece further punched with a 1.5 mm dispensing needle (Jensen Global 14 Gauge, Howard Electronic Instrument, El Dorado, KS) to create the input/output ports. The fluidic connectors were placed on top of the inlet and outlet, and 5 μL of liquid PDMS was poured on the edge of the connectors. Afterward, the chip was incubated for 5 h on a hotplate (80 °C) to fix the connectors and remove air gaps between layers. The microfluidic device was sterilized using autoclaving prior to conducting experiments (catalog #OAA50X120, All American Canner, Hillsville, VA).

Patterning the Agarose Membrane. The mask design was printed on a transparency film using a wax printer (Xerox ColorQube 8570, Xerox Corporation, Norwalk, CT). Unsolidified PDMS mixture was prepared, poured over the printed transparency film, and cured on a hot plate (80 °C for 5 h) to complete the PDMS mold. An array of hollow circles (diameter = 2 cm) were cut in the double-sided tape and attached to the glass slide to create wells. Approximately 2 mg of agarose powder was melted in 100 mL of deionized water and poured over the wells to achieve a uniform membrane thickness. With the agarose solution still in the aqueous state, the PDMS mold was placed on top of the agarose. After 5 min, the PDMS mold was removed which left extrusions on the surface of the agarose membrane (Figure 1a).

Generation and Optimization of a Concentration Gradient. To verify the establishment of a chemical gradient in the agarose membrane, two enclosed parallel channels were prepared in double- sided tape that incorporated circular holes on their ceiling (Figure 1a). Fluorescein solution (30 μM) was introduced in one channel while lysogeny broth (LB) growth media was introduced in the other channel (both flow rates = 0.02 mL h^{-1}). A thin agarose membrane was placed between the parallel channels, overlapping the circular holes. The device was positioned on a heating plate to maintain a constant temperature (37 °C) and fluorescence images were captured for 12 h at 1 h intervals. The two solutions diffused into the agarose membrane to form a steady concentration gradient. Fluorescence intensities were measured using ImageJ software and the relative fluorescein concentrations in the agarose membrane were quantified. Bacterial Strains and Sample Preparation. For all cell growth and antimicrobial susceptibility assays, derivatives of the *Escherichia coli* K-12 strain MG1655 were used. For CRISPRi experiments we utilized the *rph*$^{+}$ derivative of MG1655 BW30270 (obtained from the Coli Genetic Stock Center, Yale University) that was engineered by integrating a DNA construct where the gene expressing dCas9 under control of a tetracycline inducible promoter was integrated into the bacterial chromosome, as described,[30] resulting in strain NB125. A ColE1-like plasmid[11] was constructed to constitutively express a single-guide RNA gene targeting the *ftsZ* gene promoter region and introduced into NB125 by transformation. For all experiments, a single colony was selected to inoculate 5 mL of LB in a sterile culture tube and incubated at 37 °C for 12−18 h with shaking at 250 rpm in a benchtop incubator. After incubation, 100 μL of *E. coli* was diluted in 5 mL of LB within a 15 mL culture tube, mixed thoroughly by vortexing, and incubated at 37 °C with agitation for 2 h.

Autofocusing Module. An autofocusing module was developed that automatically detects the loss in image focus and mechanically adjusts the focus knob of the microscope. The hardware of the autofocusing system consisted of a microcontroller (Arduino UNO), a stepper motor (ROB-09238), a motor driver (Adafruit 1438), and a customized gear (Digi-Key Corporation, Thief River Fall, MN) (Figure 2b). The autofocusing Matlab script initially instructed the camera to capture 10 images at different focal planes. The focus measure F of these images was calculated using the following equation[31]

where $g(x,y)$ represents the mean intensity of the grayscale image at position coordinates (x,y) with $M \times N$ pixels (Figure 3). Similarly, $g(x$

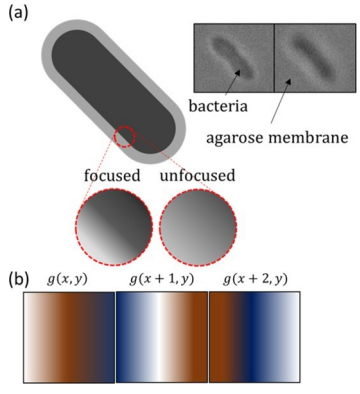

Figure 3. Working principle of the autofocusing module. (a) Blurring of the cell membrane under focused and unfocused conditions are shown (red circle), along with actual images of a bacterial cell at 100× magnification. (b) Focus measure (F) is calculated from the image intensities at three positional coordinates to estimate the blurriness of the current image.

DOI: 10.1021/acssensors.9b0103

$+ 1,y)$ and $g(x + 2,y)$ denote the mean intensities at position coordinates $(x + 1,y)$ and $(x + 2,y)$, respectively. The F value was maximum for focused images (Figure 3). After the maximum F value was identified, information regarding the number of rotational steps for the focus knob was relayed to the microcontroller. The stepper motor was actuated to rotate the focus knob. The above procedure was repeated periodically for the length of the experiment.

Inoculation and Cell Growth in the Microfluidic Platform. The bacterial sample (0.1 μL) (approximately 1000 cells) was dispensed on top of the extruded agarose membrane using a syringe (Hamilton liquid handling, online vendor). Incubation for 5−10 min allowed for membrane absorption and immobilization of bacterial cells on the agarose surface. After placing the coverslip, a sealant (CytoBond Coverslip Sealant, SciGene, Sunnyvale, CA) was poured on the edge of the coverslip for fixation and to minimize evaporation. Time-lapse images of bacterial growth were recorded using a phase contrast 100× objective lens every 20 min for 10 h. The environmental chamber and objective heater were used to maintain a temperature between 36 and 37 °C. The LB growth media were provided to the microfluidic device at a steady flow rate (0.04 mL

$$F = \sum_{x=1}^{M-1}\sum_{y=1}^{N} g(x, y)g(x + 1, y) - \sum_{x=1}^{M-2}\sum_{y=1}^{N} g(x, y)g(x + 2, y) \quad (1)$$

h^{-1}).

RESULTS AND DISCUSSION

Method Validation for Cell Growth and Autofocused Imaging. We tracked the growth dynamics of single *E. coli* cells on the agarose membrane (in LB media) for up to 425 min ($N = 3$). Consistent cell doubling time characteristic of logarithmic phase growth was observed throughout the time course (Figure 4). Because variations in the focal plane can occur due to the weight of the objective lens, the autofocusing module periodically adjusted the depth map (the distance between the objects and the optical lens) to maintain the image focus for long time periods.

Next, we tested the effects of antibiotics on the cultured bacteria. β-Lactam class antibiotics are widely used to treat bacterial infections and function by inhibiting cell wall biosynthesis.[32] We administered ampicillin (or amoxicillin) to *E. coli* cultured with continuous delivery of LB growth medium on the agarose membrane at 37 °C. Over the course of 3 h we monitored the cell morphology during exposure to the two antibiotics (5 mg/L of amoxicillin and 5 mg/L of ampicillin) (Figure 5).

DOI: 10.1021/acssensors.9b0103

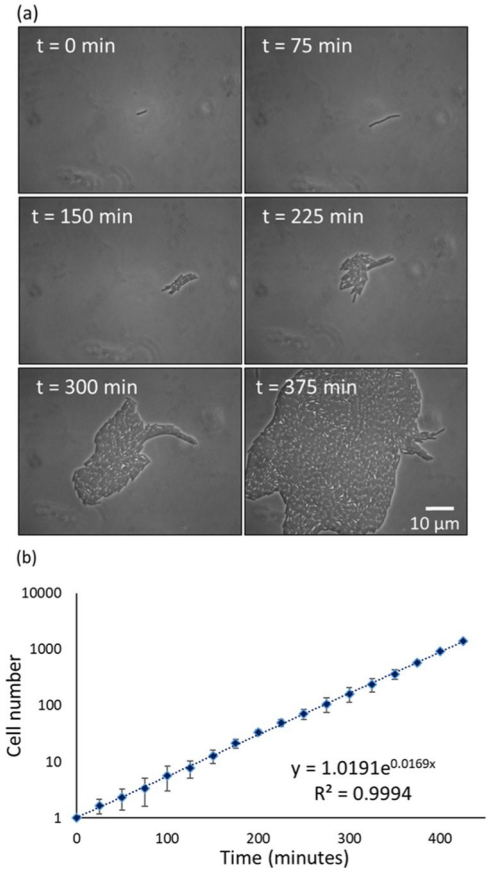

Figure 4. Measuring *E. coli* growth on the microfluidic platform. (a) Time-lapsed images of a single bacterial cell growing on the agarose membrane of the device for 425 min. The growth media was continuously provided by the microfluidic channels. The autofocusing module maintained the image focus and quality throughout the experiment. (b) ImageJ was used to obtain the bacterial cell count from the recorded images during three independent experimental runs.

Shortly after the initial exposure of amoxicillin, bacterial growth halted. After continued exposure to amoxicillin, bacterial cell division was interrupted as evidenced by cell elongation, followed by cell lysis at 25 min (Figure 5a). This observation was consistent with the action of the β-lactam antibiotics.[32] During ampicillin exposure, we also observed distinct differences to the cell shape, including initial bulging at the cell wall and spheroplast formation by 50 min (Figure 5b). Cell lysis and death occurred much later in ampicillin (compared to amoxicillin) at 250 min postexposure. This experiment showed that the microfluidic platform was capable of effective administration of antibiotics, along with fine- resolution image acquisition to discern morphological changes in cells.

Determining Antibiotic Susceptibility with Gradient Microfluidics. Next, we sought to determine MIC of ampicillin against *E. coli*. A concentration gradient of the antibiotic, if established in the agarose membrane, could directly reveal MIC levels. To quantify the antibiotic concentrations in the chemical gradient device, we used fluorescein as a representative molecule with similar molecular weight as ampicillin. Because the diffusion rates of these compounds are comparable, we were able to back-calculate the antibiotic concentrations at specific distances with respect to time. The diffusion rates of fluorescein through the agarose membrane were measured by the fluorescence microscope. After administration of the fluorescein solution to the microfluidic device, fluorescent time-lapse imaging revealed the formation of a continuous gradient over a 12 h period (Supporting Information S1). The spatio-temporal data were used to determine the fluorescein concentrations at various distances in the agarose membrane at different time points. These results suggested that ampicillin concentration gradients could be established in our device for the determination of MICs.

To evaluate the effectiveness of the gradient microfluidic platform for quantifying antibiotic susceptibility, we observed *E. coli* cell morphology during their exposure to ampicillin over an 11 h period. Cells were first inoculated into three separate extruded stages of the agarose membrane, followed by the introduction of ampicillin (32 μg/mL) through the micro- fluidic channels. We monitored cell growth on the three extruded agarose stages for the first 5 h at 10× magnification before bactericidal levels of ampicillin diffused through the membrane. The frequency of cell division began decreasing by hour 5 for cells within the first and second extruded stages (Figure 6). Single-cell imaging was performed (100× magnification) at 3 separate distances within each extruded stage for the remaining 6 h to observe morphological changes previously observed in response to ampicillin exposure (Figure

DOI: 10.1021/acssensors.9b0103

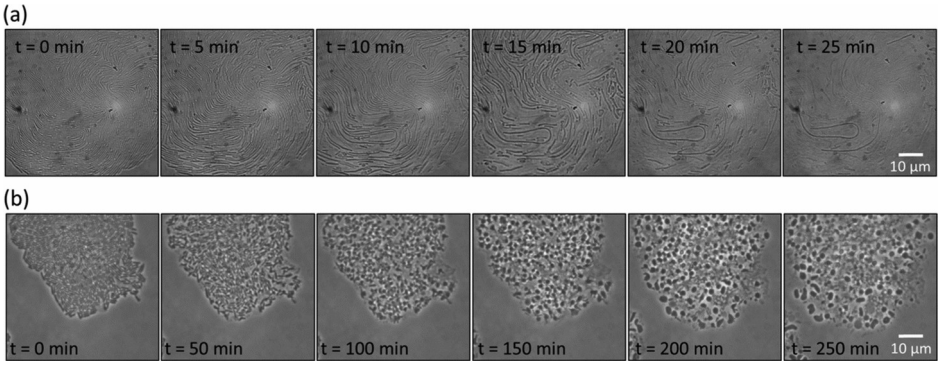

Figure 5. Morphological changes in the bacterial microcolonies exposed to two antibiotic solutions (i.e., amoxicillin and ampicillin). (a) Bacteria in early growth phase were exposed to amoxicillin solution for 2 h. Cell filamentation (i.e., elongation while maintaining a constant width) was observed which culminated in cell lysis. (b) Bacteria in the early growth phase was exposed to ampicillin solution for 2 h. This resulted in the formation of visible bulges within the cell bodies with eventual cell lysis.

DOI:
10.1021/acssensors.9b0103

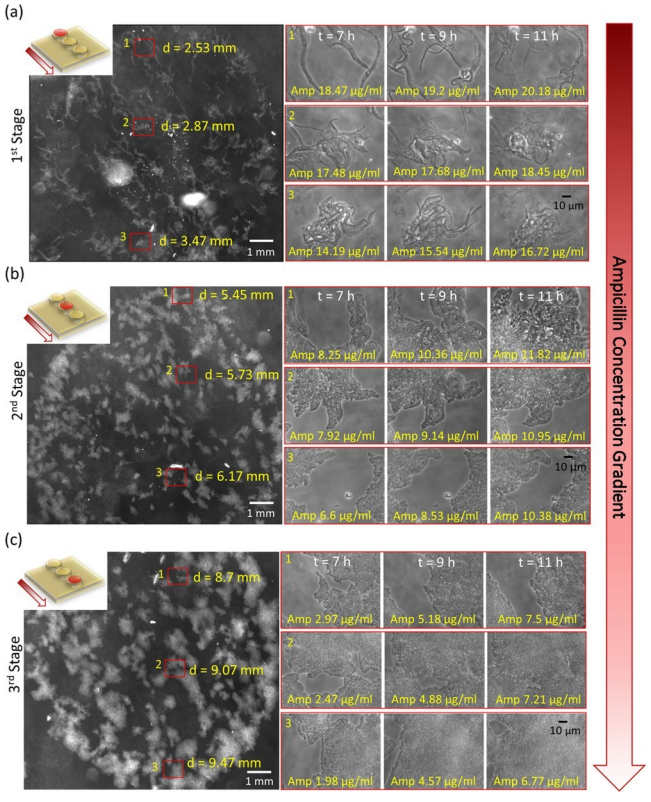

Figure 6. Measurements of the inhibitory effect of ampicillin. Bacterial cells were cultured on each extruded stage of the agarose membrane (shown in red within the insets). An ampicillin solution (32 μg/mL) was supplied through the left channel while LB growth medium was passed through the right channel. A concentration gradient of ampicillin was established in the agarose membrane. A 10× objective lens was used to monitor the bacterial colonies on the three extruded stages every hour. A 100× oil immersion objective lens was used to capture zoomed-in images of morphological changes at three distinct locations within each extruded stage. (a) First extruded stage was closer to left channel, and hence had higher ampicillin concentrations (>15 μg/mL). Images at the three locations (b1, b2, and b3) within the first stage revealed cell filamentation (up to 7 h) and eventual lysis (up to 11 h). (b) Second extruded stage had intermediate ampicillin concentrations (6.6−11.82 μg/mL). Images at the three locations (c1, c2, and c3) within the second stage revealed a clear partition between colonies exhibiting cell filamentation or normal growth (e.g., 11.82 μg/mL). (c) Third extruded stage had lower ampicillin concentrations (<7.5 μg/mL). Images at the three locations (d1, d2, and d3) revealed normal cell growth.

5b). There was cell elongation and near-complete cell lysis in the first stage where the calculated ampicillin concentrations were greater than 16 μg/mL (Figure 6a). The second stage revealed a distinct delineation of cells∂exhibiting bulging and spheroplast formation by hour 9 with more severe morphological changes observed by hour 11 (Figure 6b). In contrast, cells in the third stage furthest from the ampicillin gradient displayed no aberrant morphologies (Figure 6c).

Data from three independent experiments revealed that bactericidal effects resulted when the antibiotic concentration reached 11.82 μg/mL. Previous studies using standard antibiotic susceptibility test (AST) reported ampicillin MICs for MG1655 *E. coli* ranging from 8 to 16 μg/mL, which agrees with our findings.[4,6] The small discrepancies in the MIC values between our experiments and those reported earlier could result from differences in the bacterial strain, media

DOI: 10.1021/acssensors.9b0103

composition, growth conditions, inoculum size, readout time points, and changing gradients over time.

Use of CRISPRi in Microfluidics. We tested the feasibility of establishing gradients of chemical inducers of gene expression for the purpose of "tuning" the transcriptional activity over a defined range. For this, we incorporated CRISPRi technology into the gradient microfluidic platform to "repress" transcriptional activity of genes over a predetermined range. CRISPRi employs a nuclease-defective Cas9 protein (dCas9) and programmable guide-RNA to target the dCas9 protein toward selected DNA sequences in order to block transcription by physically interfering with RNA polymerase.[11] This technique holds several advantages over the use of conventional gene knock-out libraries, including rapid analysis of gene function requiring only construction of plasmid-based guide-RNAs, and the ability to reverse gene repression during time course experiments. CRISPRi also affords the opportunity to conditionally repress essential genes, allowing for inter- rogation of potential novel targets involved in AMR and susceptibility.[13]

To effectively regulate expression of essential genes by CRISPRi requires that dCas9 be controlled by inducers at well-defined concentrations. The exact concentrations of inducers needed are difficult to determine in plate assays, however. Consequently, we utilized our microfluidic device to establish a gradient of anhyrotetracycline (aTc). This inducer of gene expression works by allosterically binding to the TetR repressor protein to prevent its binding to the *tet* operator sequences, and is functional in a wide variety of organisms.[33] For this study, we used the *E. coli* strain NB125, which was engineered to express dCas9 from the *tet* promoter element, as described in the Materials and Methods section. This strain also expressed a guide RNA designed to target the essential *ftsZ* gene for repression by CRISPRi.[34] It is well established that depletion of the FtsZ protein impairs normal cell division, resulting in increasing cell length and eventual cell death in bacteria.[13,26]

Using the microfluidic gradient device, we inoculated *E. coli* strain NB125 on the three extruded stages of the agarose membrane, followed by the introduction of aTc solution (10 μg/mL) to establish a gradient of the inducer. The aTc concentrations (MW: 426.4 g/mol) on the agarose membrane were back-calculated from the fluorescein gradient curves (MW: 332.3 g/mol) (Supporting Information S1). We observed morphological changes in the cells within the first hour at the highest aTc concentrations (1.27 μg/mL) which was consistent with the hypothesis of FtsZ protein depletion. Continued incubation in high concentrations of aTc for 3 h resulted in extreme cell elongation (Figure 7a, bottom row). Exposure to intermediate concentrations of aTc revealed additional morphological changes consistent with an inter- mediate state of dCas9 repression, as a more modest elongated morphology was observed in a majority of cells (Figure 7a, middle row). Low concentrations of the inducer, however, did not affect cell growth or cell division (Figure 7a, top row). In contrast, no observable changes in cell shape were observed in the aTc gradient using cells transformed with a control plasmid that did not express a sequence specific guide-RNA (Figure 7b). The results of this experiment confirmed that incremental repression of targeted genes is achievable using CRISPRi in combination with gradient microfluidics devices. Our proof of concept holds promise for leveraging the high-throughput abilities of both microfluidics and CRISPRi to characterize new

DOI: 10.1021/acssensors.9b0103

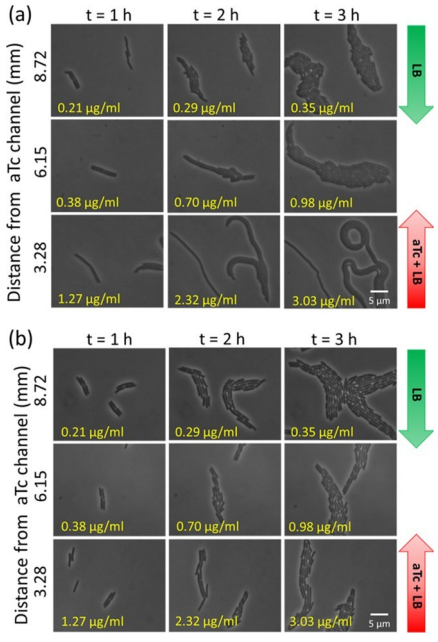

Figure 7. Morphological changes in bacteria resulting from the ftsZ gene repression by CRISPRi. LB media was supplied through the left channel while the inducer solution (aTc and LB media) was provided through the right channel. A concentration gradient of the inducer was established in the agarose membrane. (a) Cell filamentation was observed in regions where the aTc concentration exceeded 0.7 μg/ mL. Cell division was no longer observed in locations where the aTc concentration was higher than 1.2 μg/mL. (b) Normal cell growth (with no inhibition of cell division) was observed in control experiments where bacterial cells expressing a nontargeting guide- RNA were exposed to aTc inducer.

AMR genetic determinants and their associated phenotypes[13] in a variety of microbial species, which is more challenging using standard culturing and microscopic techniques.

This approach will allow us to address questions that distinguish between the phenomena of resistance, persistence, or tolerance to antibiotics.[1,6] Specifically, these studies can benefit from the long-term imaging conditions required to characterize the system noise.[11−13,33] Experiments to address these questions can benefit from platforms where rapid results could be obtained in a time- and cost-effective manner. In addition, the available antimicrobial susceptibility test (AST) (e.g., disc diffusion and broth dilution tests) require a larger number of tests to determine the MIC that are costly and time-intensive.[1,2] Our gradient chips provide a viable alternative to AST tests where a single run can provide results on the MIC and antibiotic susceptibility. The presented microfluidic platform could be expanded to study effects of combinations of chemicals (i.e., inducers, bactericidal or bacteriostatic antibiotics, growth media)[35] and gene-silencing targets on bacterial cell growth and division with valuable information on their resistance or tolerance levels.[3,5,26] The throughput of the presented platform could be improved by increasing the agarose membrane area, adding more extruded stages, and incorporating an automated $X-Y$ positioning stage. Because the adhesive tapes and transparency films are scribed using a cutting machine, there is scope to increase the spatial area of the culture platform.

Besides phenotypic growth-based testing of resistance, a number of rapid AST technologies have been recently reported

DOI: 10.1021/acssensors.9b0103

using DNA amplification of targeted genes, immunochroma- tography, and antibiotic degradation assays.[36−38] A digital real- time nucleic acid quantification assay was developed using loop-mediated isothermal amplification to detect bacteria in urine samples.[37] Optical growth of bacterial cells has been estimated by the use of pH indicators, redox indicators, luciferase phage indicators, ATP bioluminescence, and flow cytometry.[36] Ultrasensitive bacterial growth assays have also been developed by incubating cells in microdroplets and using the matrix-assisted laser desorption ionization time-of-flight mass spectroscopy technique to analyze bacterial isolates that can hydrolyze antibiotics and exhibit resistance.[39] Isolation of bacteria from whole blood and subsequent profiling of growth has been accomplished by cell-sorting techniques such as inertial focusing .[39] Whole genome sequencing has been used to identify single resistance mechanisms through measuring associated gene expressions levels. These genotypic tests are not generalizable to different pathogens or different mecha- nisms of resistance.[37] While progress in alternative AST techniques is indeed commendable, the phenotypic growth- based testing is still universally applicable and independent of the mechanism of resistance. Phenotypic ASTs directly measures the inhibition of bacterial cell growth by an antibiotic. Because of this reason, phenotypic testing has applicability in clinical settings where the standard parameters are cell growth and division in overnight cultures. The limitations of the growth-based assays, as the one presented here, are the inherent lag time for cell growth and diffusion of antibiotics through membranes which limits the detection limit to few hours. As such, while our platform is not suited for rapid AST diagnostics where the desired detection time is needed within 15−30 min, it can provide an added layer of validation for results obtained from existing rapid AST methods.[36,38,39] In addition, considering the costs of fabricating complicated microfluidics[38] and using molecular detection tools for AST markers,[37] our method uses low-cost materials and imaging system for long-term phenotypic characterization of resistance which is a valuable attribute in resource-limited settings.

CONCLUSIONS

The microfluidic platform described here enabled real-time, long-term imaging of bacterial cells (single cells and small populations). Compared to silicon and PDMS microfluidics, the device fabrication cost is considerably low by choosing inexpensive materials and cutting tools, which would help in the wider adoption of this platform for microbiology. The device design leveraged some of the benefits of open systems (i.e., Petri dishes and multiwell plates), fluid flow systems (i.e., PDMS microfluidics), and encapsulated systems (i.e., droplet microfluidics). A benchtop student microscope was modified with an environmental chamber and autofocusing module to allow real-time recording of bacterial cells for over 10 h. Continuous perfusion of media and antibiotics helped establish the desired concentration gradients of chemicals to observe single cell growth and division. Different morphological changes in response to varying concentrations of antibiotics were recorded that can be a rapid screen for antibiotic susceptibility. We further showed that the platform was effectively used for CRISPRi inhibition of cell division by repressing the essential *ftsZ* gene. This general approach can be used to screen for both essential and nonessential bacterial genes that enhance the effectiveness of antibiotics.

DOI: 10.1021/acssensors.9b0103

ASSOCIATED CONTENT

Supporting Information

The Supporting Information is available free of charge on the ACS Publications website at DOI: 10.1021/acssen- sors.9b01031.

Diffusion tests with fluorescein (PDF)

Real-time video of bacterial cell growth (AVI) Inhibitory effects of amoxicillin (AVI) Inhibitory effects of ampicillin (AVI)

AUTHOR INFORMATION

Corresponding Authors

*E-mail: gregory@iastate.edu (G.J.P.).

*E-mail: pandey@iastate.edu (S.P.).

ORCID

Christopher Legner: 0000-0002-8617-7653

Author Contributions

§T.K. and N.B. contributed equally to this work.

Notes

The authors declare no competing financial interest.

ACKNOWLEDGMENTS

This work was supported by the Defense Threat Reduction Agency (HDTRA1-11-16-BRCWMD-BAA) and the U.S. National Science Foundation [NSF IDBR-1556370].

REFERENCES

(1) Liu, Z.; Banaei, N.; Ren, K. Microfluidics for Combating Antimicrobial Resistance. *Trends Biotechnol.* 2017, *35*, 1129−1139.

(2) Liu, Z.; Sun, H.; Ren, K. A Multiplexed, Gradient-Based, Full- Hydrogel Microfluidic Platform for Rapid, High-Throughput Antimicrobial Susceptibility Testing. *Chempluschem* 2017, *82*, 792−
801.

(3) Rusconi, R.; Garren, M.; Stocker, R. Microfluidics Expanding the Frontiers of Microbial Ecology. *Annu. Rev. Biophys.* 2014, *43*, 65−91.

(4) Tashiro, Y.; Eida, H.; Ishii, S.; Futamata, H.; Okabe, S. Generation of Small Colony Variants in Biofilms by Escherichia Coli Harboring a Conjugative F Plasmid. *Microbes Environ.* 2017, *32*, 40− 46.

(5) Goverdhana, S.; Puntel, M.; Xiong, W.; Zirger, J. M.; Barcia, C.;
Curtin, J. F.; Soffer, E. B.; Mondkar, S.; King, G. D.; Hu, J.; et al. Regulatable Gene Expression Systems for Gene Therapy Applications: Progress and Future Challenges. *Mol. Ther.* 2005, *12*, 189−211.

(6) Ibacache-Quiroga, C.; Oliveros, J. C.; Couce, A.; Blaźquez, J.
Parallel Evolution of High-Level Aminoglycoside Resistance in Escherichia Coli Under Low and High Mutation Supply Rates. *Front. Microbiol.* 2018, *9*, 427.

(7) Sun, P.; Liu, Y.; Sha, J.; Zhang, Z.; Tu, Q.; Chen, P.; Wang, J. High-Throughput Microfluidic System for Long-Term Bacterial Colony Monitoring and Antibiotic Testing in Zero-Flow Environ- ments. *Biosens. Bioelectron.* 2011, *26*, 1993−1999.

(8) Kaminski, T. S.; Scheler, O.; Garstecki, P. Droplet Microfluidics for Microbiology: Techniques, Applications and Challenges. *Lab Chip* 2016, *16*, 2168−2187.

(9) Lycke, R.; Parashar, A.; Pandey, S. Microfluidics-Enabled Method to Identify Modes of Caenorhabditis Elegans Paralysis in Four Anthelmintics. *Biomicrofluidics* 2013, *7*, 064103.

(10) Wang, T.; Guan, C.; Guo, J.; Liu, B.; Wu, Y.; Xie, Z.; Zhang, C.; Xing, X.-H. Pooled CRISPR Interference Screening Enables Genome- Scale Functional Genomics Study in Bacteria with Superior Performance. *Nat. Commun.* 2018, *9*, 2475.

(11) Qi, L. S.; Larson, M. H.; Gilbert, L. A.; Doudna, J. A.; Weissman, J. S.; Arkin, A. P.; Lim, W. A. Repurposing CRISPR as an

DOI: 10.1021/acssensors.9b0103

RNA-Guided Platform for Sequence-Specific Control of Gene Expression. *Cell* 2013, *152*, 1173−1183.
(12) Rousset, F.; Cui, L.; Siouve, E.; Becavin, C.; Depardieu, F.; Bikard, D. Genome-Wide CRISPR-DCas9 Screens in E. Coli Identify Essential Genes and Phage Host Factors. *PLoS Genet.* 2018, *14*, No. e1007749.
(13) Peters, J. M.; Colavin, A.; Shi, H.; Czarny, T. L.; Larson, M. H.;
Wong, S.; Hawkins, J. S.; Lu, C. H. S.; Koo, B.-M.; Marta, E.; et al. A Comprehensive, CRISPR-Based Functional Analysis of Essential Genes in Bacteria. *Cell* 2016, *165*, 1493−1506.
(14) Deutmeyer, A.; Raman, R.; Murphy, P.; Pandey, S. Effect of magnetic field on the fermentation kinetics of Saccharomyces cerevisiae. *Adv. Biosci. Biotechnol.* 2011, *02*, 207−213.
(15) Kim, S.; Cestellos-Blanco, S.; Inoue, K.; Zare, R. Miniaturized Antimicrobial Susceptibility Test by Combining Concentration Gradient Generation and Rapid Cell Culturing. *J. Antibiot.* 2015, *4*, 455−466.
(16) Haessler, U.; Kalinin, Y.; Swartz, M. A.; Wu, M. An Agarose- Based Microfluidic Platform with a Gradient Buffer for 3D Chemotaxis Studies. *Biomed. Microdevices* 2009, *11*, 827−835.
(17) Li, Y.; Yan, X.; Feng, X.; Wang, J.; Du, W.; Wang, Y.; Chen, P.;
Xiong, L.; Liu, B.-F. Agarose-Based Microfluidic Device for Point-of- Care Concentration and Detection of Pathogen. *Anal. Chem.* 2014, *86*, 10653−10659.
(18) Qiu, Y.; Zhang, J.; Li, B.; Wen, X.; Liang, P.; Huang, X. A Novel Microfluidic System Enables Visualization and Analysis of Antibiotic Resistance Gene Transfer to Activated Sludge Bacteria in Biofilm. *Sci. Total Environ.* 2018, *642*, 582−590.
(19) Bielecka, M. K.; Tezera, L. B.; Zmijan, R.; Drobniewski, F.; Zhang, X.; Jayasinghe, S.; Elkington, P. A Bioengineered Three- Dimensional Cell Culture Platform Integrated with Microfluidics to Address Antimicrobial Resistance in Tuberculosis. *mBio* 2017, *8*, No. e02073-16.
(20) Eun, Y.-J.; Utada, A. S.; Copeland, M. F.; Takeuchi, S.; Weibel,
D. B. Encapsulating Bacteria in Agarose Microparticles Using Microfluidics for High-Throughput Cell Analysis and Isolation. *ACS Chem. Biol.* 2011, *6*, 260−266.
(21) Kim, K.; Kim, S.; Jeon, J. S. Visual Estimation of Bacterial Growth Level in Microfluidic Culture Systems. *Sensors* 2018, *18*, 447.
(22) Beeman, A. Q.; Njus, Z. L.; Pandey, S.; Tylka, G. L. Chip Technologies for Screening Chemical and Biological Agents Against Plant-Parasitic Nematodes. *Phytopathology* 2016, *106*, 1563−1571.
(23) Njus, Z.; Feldmann, D.; Brien, R.; Kong, T.; Kalwa, U.; Pandey,
S. Characterizing the Effect of Static Magnetic Fields on C. elegans Using Microfluidics. *Adv. Biosci. Biotechnol.* 2015, *06*, 583−591.
(24) Carr, J. A.; Lycke, R.; Parashar, A.; Pandey, S. Unidirectional, Electrotactic-Response Valve for Caenorhabditis Elegans in Micro- fluidic Devices. *Appl. Phys. Lett.* 2011, *98*, 143701.
(25) Kong, T.; Brien, R.; Njus, Z.; Kalwa, U.; Pandey, S. Motorized Actuation System to Perform Droplet Operations on Printed Plastic Sheets. *Lab Chip* 2016, *16*, 1861−1872.
(26) Li, X.-t.; Jun, Y.; Erickstad, M. J.; Brown, S. D.; Parks, A.; Court,
D. L.; Jun, S. TCRISPRi: Tunable and Reversible, One-Step Control of Gene Expression. *Sci. Rep.* 2016, *6*, 39076.
(27) Hsieh, K.; Zec, H. C.; Chen, L.; Kaushik, A. M.; MacH, K. E.; Liao, J. C.; Wang, T. H. Simple and Precise Counting of Viable Bacteria by Resazurin-Amplified Picoarray Detection. *Anal. Chem.* 2018, *90*, 9449−9456.
(28) Kaushik, A. M.; Hsieh, K.; Chen, L.; Shin, D. J.; Liao, J. C.; Wang, T.-H. Accelerating Bacterial Growth Detection and Anti- microbial Susceptibility Assessment in Integrated Picoliter Droplet Platform. *Biosens. Bioelectron.* 2017, *97*, 260−266.
(29) Scheler, O.; Pacocha, N.; Debski, P. R.; Ruszczak, A.; Kaminski,
T. S.; Garstecki, P. Optimized Droplet Digital CFU Assay (DdCFU) Provides Precise Quantification of Bacteria over a Dynamic Range of 6 Logs and Beyond. *Lab Chip* 2017, *17*, 1980−1987.
(30) Shanmugam, S. K.; Backes, N.; Chen, Y.; Belardo, A.; Phillips,
G. J.; Dalbey, R. E. New Insights into Amino-Terminal Translocation

DOI:
10.1021/acssensors.9b01033

as Revealed by the Use of YidC and Sec Depletion Strains. *J. Mol. Biol.* 2019, *431*, 1025−1037.
(31) Price, J. H.; Gough, D. A. Comparison of Phase-Contrast and Fluorescence Digital Autofocus for Scanning Microscopy. *Cytometry* 1994, *16*, 283−297.
(32) Yao, Z.; Kahne, D.; Kishony, R. Distinct Single-Cell Morphological Dynamics under *β*-Lactam Antibiotics. *Mol. Cell* 2012, *48*, 705−712.
(33) Ehrt, S.; Guo, X. V.; Hickey, C. M.; Ryou, M.; Monteleone, M.; Riley, L. W.; Schnappinger, D. Controlling Gene Expression in Mycobacteria with Anhydrotetracycline and Tet Repressor. *Nucleic Acids Res.* 2005, *33*, No. e21.
(34) Zhou, P.; Helmstetter, C. E. Relationship between FtsZ Gene Expression and Chromosome Replication in Escherichia Coli. *J. Bacteriol.* 1994, *176*, 6100−6106.
(35) Ding, X.; Njus, Z.; Kong, T.; Su, W.; Ho, C.-M.; Pandey, S. Effective Drug Combination for Caenorhabditis Elegans Nematodes Discovered by Output-Driven Feedback System Control Technique. *Sci. Adv.* 2017, *3*, No. eaao1254.
(36) Idelevich, E. A.; Becker, K. How to Accelerate Antimicrobial Susceptibility Testing. *Clin. Microbiol. Infect.* 2019, DOI: 10.1016/ j.cmi.2019.04.025.
(37) Schoepp, N. G.; Schlappi, T. S.; Curtis, M. S.; Butkovich, S. S.; Miller, S.; Humphries, R. M.; Ismagilov, R. F. Rapid Pathogen-Specific Phenotypic Antibiotic Susceptibility Testing Using Digital LAMP Quantification in Clinical Samples. *Sci. Transl. Med.* 2017, *9*, No. eaal3693.
(38) Baltekin, Ö.; Boucharin, A.; Tano, E.; Andersson, D. I.; Elf, J. Antibiotic Susceptibility Testing in Less than 30 Min Using Direct Single-Cell Imaging. *Proc. Natl. Acad. Sci. U.S.A.* 2017, *114*, 9170− 9175.
(39) Kelley, S. O. New Technologies for Rapid Bacterial Identification and Antibiotic Resistance Profiling. *SLAS Technol. Transl. Life Sci. Innov.* 2017, *22*, 113−121.

DOI: 10.1021/acssensors.9b01033